

Polymer Chemistry

Accepted Manuscript



This is an *Accepted Manuscript*, which has been through the Royal Society of Chemistry peer review process and has been accepted for publication.

Accepted Manuscripts are published online shortly after acceptance, before technical editing, formatting and proof reading. Using this free service, authors can make their results available to the community, in citable form, before we publish the edited article. We will replace this *Accepted Manuscript* with the edited and formatted *Advance Article* as soon as it is available.

You can find more information about *Accepted Manuscripts* in the [Information for Authors](#).

Please note that technical editing may introduce minor changes to the text and/or graphics, which may alter content. The journal's standard [Terms & Conditions](#) and the [Ethical guidelines](#) still apply. In no event shall the Royal Society of Chemistry be held responsible for any errors or omissions in this *Accepted Manuscript* or any consequences arising from the use of any information it contains.

ARTICLE

Cite this: DOI:
10.1039/X0XX00000X

Received 00th January 201,
Accepted 00th January 201

DOI: 10.1039/X0XX00000X

www.rsc.org/

Alkoxyamine-functionalized latex nanoparticles through RAFT polymerization-induced self-assembly in water.

Claude St Thomas,^{ab} Ramiro Guerrero-Santos^{*a} and Franck D'Agosto^{*b}

Abstract.—The use of a new symmetrical trithiocarbonate holding two alkoxyamine moieties (**I**), was explored in surfactant-free emulsion polymerization of styrene or *n*-butyl acrylate through reversible addition-fragmentation chain transfer (RAFT). **I** revealed as an effective chain transfer agent in the synthesis of well-defined end-functionalized poly(acrylic acid)s (PAA). These macro RAFT agents were further used in water for the preparation of amphiphilic triblock copolymers by polymerization induced self-assembly (PISA). The corresponding final latex particles decorated with alkoxyamine moieties were used to trigger out NMP polymerization of sodium 4-styrene sulfonate (SSNa) in water. The thermal activation of the surface alkoxyamines groups which had hitherto been dormant induced the formation of a double hydrophilic corona PAA-*b*-PSSNa and a sharp reorganization of latex particles.

Introduction

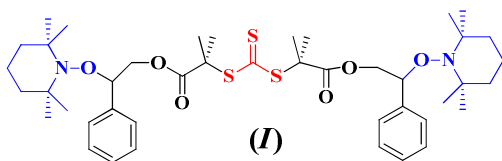
The Reversible deactivation radical polymerization RDRP¹, developed during the decade of the nineties is now a well-settled methodology to prepare macromolecular architectures exhibiting low dispersity ($D = M_w/M_n$) and predetermined molar mass (MM). The main RDRP techniques, which are also termed as controlled radical polymerizations, include nitroxide-mediated polymerization (NMP)^{2,3,4} atom transfer radical polymerization (ATRP),^{5,6} and reversible addition-fragmentation chain transfer (RAFT)^{7,8,9} polymerization. Commonly, these techniques are carried out in homogeneous media to prepare well-defined homo and block copolymers or more complex architectures. Furthermore, the implementation of RDRP in aqueous dispersed systems, especially in emulsion polymerization, has gained increasing interest due to environmental concerns and its industrial potential.¹⁰ For instance, extensive research has been reported on the use of NMP technique to synthesize homopolymers and block copolymers with controlled molar masses and low D in waterborne polymerization.^{11,12,13} However, high operating temperatures is still a significant issue as most common nitroxides or alkoxyamines operate at temperatures above 120 °C. Special attention has been received to the development of low temperature nitroxides or alkoxyamines to avoid conducting polymerizations into pressurized reactors.^{14,15}

Moreover, in the frame of RDRP in emulsion, the use of molecular controlling agents that ensure the control of the chain growth revealed to be difficult due to their localization in the different phases.¹⁶

A remarkable achievement was performed by Ferguson et al. who applied for the first time a method starting with the synthesis by RAFT of a very short poly(acrylic acid) (PAA) living polymer (five acrylic acid, AA, units) in presence of a reversible chain transfer agent.¹⁷ The living polymer was further chain-extended with a slow feed of *n*-butyl acrylate to form amphiphilic block copolymers able to self-assemble into frozen micelles in which the polymerization can further continue. Since these pioneered results, this approach has evolved in an extremely efficient and simple way of producing amphiphilic block copolymer particles by polymerization-induced self-assembly (PISA) performed in water¹⁸ or in other media¹⁹ without the use of additional surfactant. The control gained via the use of a RAFT process allows producing well-defined objects in which the nature and the functionality of the hydrophilic shell or the hydrophobic block can be tuned. Besides, the final morphology of these supra-macromolecular arrangements mainly depends on the relative volume fractions of each block as well as on the

interfacial energy created at the blocks junction. As a result, spheres but also fibers or vesicles, that can be obtained by the self-assembly of preformed amphiphilic block copolymers in selective solvents,²⁰ can also be achieved using PISA in high solids content and by tuning the reaction conditions.²¹

Recently, we have reported the synthesis of a symmetrical functionalized trithiocarbonate²² ($R = R' =$ alkoxyamine) or dithioesters²³ which were applied to the preparation of multiblock copolymers in homogeneous media via alternated or *in tandem* RAFT/NMP. As the chemical structure of both RAFT and NMP controlling agents strongly impacts their aptitude to control the polymerization of the diverse classes of monomers, the use of such double-headed molecules opens a new way to produce unique polymer structures.



Scheme 1. Structure of the double headed alkoxyamine trithiocarbonate (**I**).

The potential use of these new thiocarbonylthio compounds in aqueous dispersed systems has not been reported yet. Based on the above mentioned PISA strategy, we anticipated that the RAFT synthesis of hydrophilic living polymers mediated by **I** would give excellent candidates to generate original amphiphilic triblock copolymer particles. The presence of the alkoxyamine moieties that could keep their integrity during the RAFT process may remain at the surface of the final particles providing a unique and unreported way of achieving surface alkoxyamine functionalized latex particles. Further use of these alkoxyamine groups to initiate NMP from the particle surface (surface initiated polymerization, SIP) may lead to interesting new morphologies.

In this paper, we describe the preparation of well-defined α,ω -dialkoxyamine poly(acrylic acid) trithiocarbonate using the symmetrical dialkoxyamine-functionalized trithiocarbonate **I** (see Schemes 1 and 2). This trifunctional polymer was subsequently utilized in a surfactant-free RAFT emulsion polymerization of styrene or *n*-butyl acrylate. Lastly, the latexes were charged with sodium 4-styrenesulfonate and heated to trigger out SIP via dissociation of alkoxyamine end-groups located at the outer layer of the PAA hydrophilic corona.

2. Experimental

2.1 Materials

Acrylic acid (AA, Acros, 99.9%), 4,4'-azobis(4-cyanopentanoic acid) (ACPA, Fluka, >98%), sodium hydrogen carbonate (NaHCO_3 , Aldrich, >99%), sodium 4-styrene sulfonate (SSNa, Aldrich, 99.5%), tetrahydrofuran (THF, Fluka HPLC, 99.5%), deuterium oxide (D_2O , Aldrich, 99.9 atom %D), dimethyl sulfoxide (DMSO- d_6 , Aldrich, 99.9 atom %D), and trimethylsilyl diazomethane (Fluka, 99.5%) were used as received. Styrene (S, Aldrich, 99%) was purified by removing the inhibitor by filtration with aluminium oxide. *n*-butyl acrylate (BA, Acros, 99%) was distilled under reduced pressure. Spectra/Por molecular porous membrane tubing (Spectrum Laboratories) was used as purchased. Water was deionized before use (Purelab classic UV, Elga LabWater). **I** was synthesized as reported previously.²²

2.2 Analysis

To determine the conversion of AA at different times, one drop of the reaction mixture was taken out with a syringe at 3 h, 4 h, 5 h, 6 h and 8 h for ^1H NMR analysis (in DMSO- d_6) at room temperature. The integration ratio of the vinyl proton resonances between 5.9-6.6 ppm and the methylene protons resonance of 1,3,5-trioxane at 5.2 ppm used as internal reference was used to determine the monomer conversion. During the synthesis of the particles, the consumption of the hydrophobic monomer was followed by gravimetric analyses of samples withdrawn from the polymerization medium at different times.

Size exclusion chromatography (SEC) measurements were performed in THF at 40 °C at a flow of 1 mL min^{-1} with a concentration of 3 mg mL^{-1} . Before analysis polymers were modified by methylation trimethylsilyl diazomethane as a derivatization agent adapting a published protocol²⁴ and, filtrated through a 0.45 μm pore size membrane. Separation was carried out on three Polymer Laboratories columns [3 x PLgel 5 μm Mixed C (300 x 7.5 mm) and a guard column (PL gel 5 μm)]. The setup (Viskotec TDA 305) was equipped with a refractive index (RI) detector ($\lambda = 930$ nm). The average molar masses (number-average molar mass M_n and weight-average molar mass M_w) and the dispersity ($D = M_w/M_n$) were derived from RI signal by a calibration curve based on poly (methyl methacrylate) standards (PMMA from Polymer Laboratories). The same procedure was used for SEC measurements of block copolymers, using a calibration curve based on polystyrene (PS from Polymer Laboratories).

Dynamic light scattering (DLS, Nano ZS from Malvern Instruments) was used to measure the particle size (average hydrodynamic diameter, D_h) and the dispersity of samples

(Poly). Before measurements, the latex samples were diluted in deionized water.

Nuclear Magnetic Resonance (NMR) spectra were obtained in a Bruker DRX 300 in DMSO-*d*₆ and/or D₂O at room temperature.

To determine the conversion of SSNa consumed during SIP, dialysis was carried out on the final latex using molecular porous membrane tubing under vigorous magnetic agitation. Fresh water was regularly provided and conductivity measurements were used to determine when dialysis was complete. SSNa conversion was then evaluated by gravimetry performed on the water phases.

Scanning electron microscopy (SEM) images were obtained using a JEOL JSM-7401F cold type FE-SEM field emission scanning electron microscope. The sample measurements were carried out using the following procedure. The plate (copper) was cleaned with acetone and then air dried. The latexes (concentration < to 1% of solids) was drop-cast onto the surface of the plate and allowed to dry at room temperature. The surface of the films was coated with a gold and palladium alloy layer before recording the SEM images. Elemental analysis of the surface was also performed using an EDX microanalysis system.

Transmission electron microscopy (TEM) was performed at an accelerating voltage of 80 kV with a Philips CM120 transmission electron microscope at the Centre Technologique des Microstructures (CTμ), Claude Bernard University, Villeurbanne, France. Diluted samples (< 1 %) were dropped on a Formvar-carbon coated copper grid and dried under air.

In order to preserve particle shape, PBA containing latexes were observed in their natural hydrated environment using cryogenic TEM (cryo-TEM). For analysis, the sample was deposited on a continuous carbon film, blotting the water in excess, mounting the dry specimen on the Gatan holder and quenching it in liquid nitrogen before introducing in the microscope. The holder was then cooled down and the specimen was observed at -180°C. The number-average (D_n), the weight-average particle diameter (D_w), and polydispersity index ($PDI = D_w/D_n$) were calculated using $D_n = \sum n_i D_i / \sum n_i$ and $D_w = \sum n_i D_i^4 / \sum n_i D_i^3$ where n_i is the number of particles with diameter D_i .

2.3 Polymerization

Synthesis of PAA Macro RAFT agent (Step 1).

A representative experiment was carried out as follows: in a two-necked round-bottom flask equipped with a condenser 79.5 mg of **I** (0.1 mmol L⁻¹) and 5.8 mg of ACPA (2 × 10⁻² mmol L⁻¹), 3.0 mL of dioxane and 1.0 g of AA (15 mmol L⁻¹) were mixed. A small amount (0.13 mg) of 1,3,5-trioxane (1.4 mmol L⁻¹) was added as an internal reference for ¹H NMR analysis. In this particular case, the targeted M_n was 11,600 g mol⁻¹ (see Entry 6, Table 1).

The flask was degassed by bubbling argon through the solution for *ca.* 30 minutes. After this, the temperature was increased to 70 °C by immersing the flask in a thermostated oil bath. The withdrawal of samples at predetermined times allowed to follow the monomer conversion with time and the evolution of MM and \bar{D} . The formed PAA macroRAFT agents (PAA-**I**) were diluted with dioxane and precipitated out from diethyl ether. For polymerizations carried out in water a similar procedure was followed. The different PAA-**I** synthesized are listed in Table 1.

RAFT Surfactant-Free Emulsion Polymerization Procedure (Step 2).

In a typical experiment, 414 mg of styrene (3.9 mmol) and a solution of PAA-**I** (63 mg; 7.8 × 10⁻³ mmol, $M_{nSEC} = 8,040$ g mol⁻¹) in water were charged in a one-necked round bottom flask. The total volume of the reaction was adjusted with water to 5 mL. At that point, 1 mL of an aqueous solution of ACPA (concentration = 6.9 mg mL⁻¹ neutralized by 7 mol equiv of NaHCO₃) was added to the reaction mixture. The medium was degassed by bubbling argon through the solution for 30 minutes and immersed in oil bath thermostated at 80 °C (for more details see Entry L2 in Table 2). A similar procedure was followed to polymerize BA. In that case, a small amount of styrene, (< 10 %) was added in order to improve the polymerization control.²⁵ In both instances, stable latexes PAA-*b*-PS-*b*-PAA or PAA-*b*-PBA-*b*-PAA were obtained. Results are reported in Table 2.

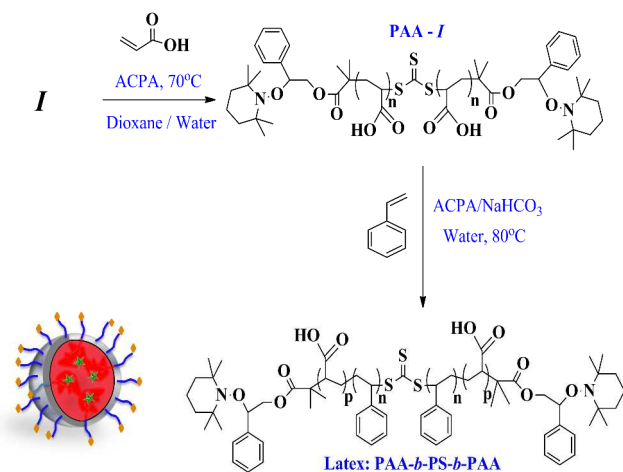
Surface Initiated Polymerization through NMP from latex nanoparticles Procedure (Step 3).

Residual monomer was removed from the latex by bubbling of argon before any SIP experiment. In a typical experiment 138 mg of SSNa (0.67 mmol L⁻¹) was added to the latex **L1** (291 mg, 7.4 × 10⁻³ mmol) described in Table 2. The mixture was charged into an autoclave reactor (50 mL), degassed with three freeze-pump-thaw cycles and heated under argon at 130°C overnight under pressure (3 bars). The dispersion obtained was characterized by TEM.

3. Results and discussion

3.1 Synthesis of PAA-I (Step 1).

The general synthetic strategy to produce stable latexes is outlined in Scheme 2. Acrylic acid RAFT polymerization was mediated by **I** to form a PAA macroRAFT agents (PAA-**I**) which were subsequently chain extended using styrene or *n*-butyl acrylate under PISA conditions at 80°C. A careful exploration on the effect of pH, concentration and molar mass of hydrophobic and hydrophilic segments over the particle size was carried out in our previous works.²⁶ Therefrom, the reactions conditions were selected as defined in the experimental section.



Scheme 2. Synthetic protocol for the preparation of alkoxyamine decorated polystyrene latex and representation of particles.

To generate the desired particles, the first step is to assess the synthesis of PAA macroRAFT using **I** as controlling agent. This can be performed in organic solvent such as dioxane.^{27, 28} As the PISA process has also been developed according to a one pot process for which both the growth of the hydrophilic and the hydrophobic segments are performed in an aqueous medium, **I**-mediated RAFT polymerization of AA was also investigated in water.²⁹ **I** being not soluble in pure water was first dissolved in AA and the resulting solution added to water. This still gave rise to aqueous suspensions that were concentrated in AA (maximum 55% v/v of water). Once the medium was heated and upon polymerization it becomes progressively clear. As it can be seen in Figure 1 polymerizations carried out in water (entries 1-3 in Table 1, $[I]/[ACPA]$ ratio of 10) were rather slow and reached 60 % conversion in 8 hours. A linear increase of molar masses versus conversion was observed from the analyses of the samples withdrawn from the polymerization reaction at different times. Low dispersity values were obtained (< 1.3) by SEC. Experimental molar mass values were higher than expected (particularly when high polymerization degrees

were targeted) which may be related the solubility problems encountered with **I** that may be slowly and not quantitatively consumed during the process. Polymerizations performed in dioxane were not associated with solubility issues of **I** and lower concentrations of AA could easily be employed (entries 4-6, Table 1). After an inhibition period was observed, around 70% conversion was reached in less than 5h when employing a $[I]/[ACPA]$ ratio of 5. Again a linear increase of the molar masses versus conversion was observed and low dispersities were obtained ($D = 1.2$). These data confirmed the controlled behaviour of the polymerizations.

SEC traces of methylated PAA-**I** (Figure S1) showed an entire shift towards lower retention times (high molar mass). However, above 50% of monomer conversion, a shoulder on the low molar mass side was systematically observed in polymerizations carried out either in water or dioxane. To obtain a better insight on the nature of this shoulder, sample PAA-**I** 2 (entry 2, $D = 1.3$ with $M_{peak} = 20,400 \text{ g mol}^{-1}$) was cleaved at the central thiocarbonylthio linkage by treatment with AIBN/PPH₃.³⁰ The SEC analysis of the resulting polymer ($M_{nSEC} = 10,220 \text{ g mol}^{-1}$ and $M_{peak} = 11,500 \text{ g mol}^{-1}$) showed that the polymer formed after cleavage was of low dispersity ($D = 1.15$) (Figure S2a) but did not seem to perfectly match the low molar mass shoulder in the initial polymer. In order to investigate this point, a deconvolution of the chromatogram of PAA-**I** 2 was performed (Figure S2b). Although very similar, the low molar mass peak obtained after deconvolution indeed mismatched the chromatogram obtained after cleavage of PAA-**I** 2. This however does not rule out a possible degradation of the middle chain trithiocarbonate moiety (i) during the polymerization due to the sensitivity of thiocarbonylthio moiety to hydrolysis in aqueous or protic media and/or (ii) during the methylation step carried out before SEC analysis.³¹ Indeed, the degradation reaction induced by treatment with the AIBN/PPH₃ may lead to PAA carrying different chain ends from the ones potentially obtained after the abovementioned degradations. The nature of these chain ends may also slightly impact the elution of the resulting polymers. Besides, the elution of mixture of two polymers is not exactly the same as the one of the same polymers analyzed alone. As these possible degradations can have serious outcomes on the success of the next emulsion polymerization step, we further performed methyl acrylate polymerization with **I** in dioxane and analyzed the polymer by SEC after a 'useless methylation' step only performed to mimic the history of our previous samples. The SEC analyses using THF as eluent and PMMA calibration standard of this PMA sample before and after methylation are reported in Figure S3. One single population of low dispersity ($M_{nSEC} = 8,800 \text{ g mol}^{-1}$, $M_{peak} =$

10,900 g mol⁻¹, $D = 1.1$) can be observed before methylation. After methylation (addition of trimethylsilyl diazomethane, 2 mL of THF and 5 drops of water), a second population of lower molar mass ($M_{nSEC} = 5,600$ g mol⁻¹, $M_{peak} = 9,800$ g mol⁻¹, $D = 1.3$) appears confirming that the methylation treatment is mainly responsible for the degradation of the trithiocarbonate linkage in the middle of the chains. This suggests that our original PAA-*I* are thus exhibiting the expected structures shown in Scheme 2.

Indeed, the ¹H NMR analysis (Figure S4) of PAA-*I* 6, confirmed the presence of the α,ω alkoxyamine- groups which is in accordance with the expected RAFT mechanism

involving *I*. ¹H NMR was also employed to calculate the molar mass of the obtained chains (M_{nNMR}) from the integration of the signals corresponding to end-groups. In this particular case, $M_{nNMR} = 8,170$ g mol⁻¹ is very close the experimental values of ($M_{nSEC} = 8,040$ g mol⁻¹). Accordingly, 98% of chains ends are capped with alkoxyamine groups stemming from *I*. This result seemed to confirm that the observed cleavage of the trithiocarbonate moiety seemed mainly to occur during the methylation of the chains.

In summary, different well-defined functionalized PAA-*I*s ($MM \leq 11$ kg mol⁻¹) were produced which were used as precursors of amphiphilic triblock copolymers through RAFT polymerization using PISA.

Table 1. RAFT polymerization of acrylic acid mediated by *I*.

Entry	PAA- <i>I</i> code	[AA] / [I]	[I] / [ACPA]	Solvent	<i>t</i> (h)	Conv ^a (%)	M_{nth}^b (g mol ⁻¹)	M_{nSEC}^c (g mol ⁻¹)	D^c
1 ^d	PAA- <i>I</i> 1	300	10	Water	7	63	14,480	10,400	1.3
2 ^d	PAA- <i>I</i> 2	300	10	Water	8	61	14,000	10,770	1.3
3 ^d	PAA- <i>I</i> 3	185	10	Water	8	49	7,340	8,040	1.2
4 ^e	PAA- <i>I</i> 4	155	4.3	Dioxane	5	77	9,400	8,820	1.2
5 ^e	PAA- <i>I</i> 5	150	5.0	Dioxane	4.5	39	5,050	4,100	1.2
6 ^e	PAA- <i>I</i> 6	150	4.5	Dioxane	5	71	8,670	8,040	1.2

^aMonomer conversion was determined by ¹H NMR. ^bTheoretical $M_n = ([AA]_0 \times \text{conversion} \times M_{AA}) / [I]_0 + M_I$ where $[AA]_0$ is molar ratio of acrylic acid (AA), $[I]_0$ is molar ratio of *I*, and M_I the molecular weight of *I*. ^cNumber-average molar mass and D determined by SEC in THF with PMMA standards. ^dCarried out in water 55% (v/v), ^eCarried out in dioxane 70% (v/v). T = 70°C.

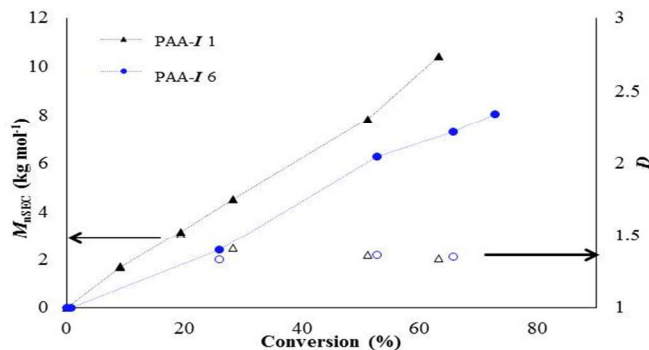


Figure 1. Conversion vs. M_{nSEC} during acrylic acid RAFT polymerization mediated by *I* at T = 70°C in water (PAA-*I* 1) or dioxane (PAA-*I* 6).

3.2 Surfactant-Free Emulsion RAFT Polymerization (Step 2).

In this step, amphiphilic block copolymers were prepared from every PAA-*I* quoted in Table 1. Emulsion polymerizations were carried out with S or BA as hydrophobic monomer at molar ratios $[M] / [PAA-I]$ in the range 400-900. ACPA was used as water soluble initiator and the pH was maintained to 3.1 as previously optimized in our group for trithiocarbonate terminated PAA macroRAFT. Table 2 summarized these different experiments.

Conversion versus time and M_{nSEC} versus conversion plots are given in Figure S5. An inhibition period (< 1h) was observed

in the case of styrene and was less pronounced in the case of BA. As already observed,²⁶ this inhibition corresponds to the very first hydrophobic monomer units that have to be incorporated to the hydrophilic macroRAFT before the latter starts to be surface active and to self-assemble. High conversion (70%) was then reached at relatively short times.

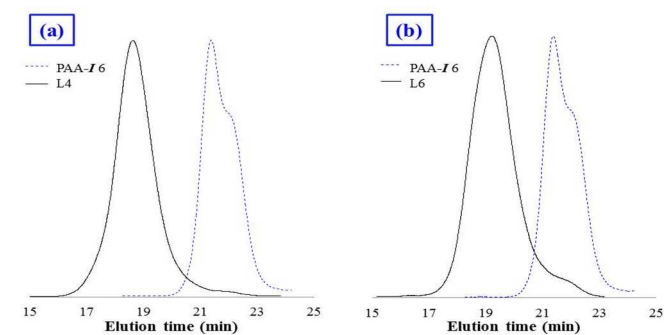


Figure 2. (a) SEC trace of PAA-*I* 6 and its corresponding block copolymer L4, (b) SEC curve of PAA-*I* 6 and its corresponding block copolymer L6.

In all cases, stable latexes were formed. As a general trend, moderate to high values of conversion were reached. As it can be seen from Figure 2, the SEC traces obtained after polymerization of S or BA showed a shift toward high molar mass in comparison with the initial PAA-*I* macro-CTA. A

noticeable increase in D (> 1.7 , see Table 2) is favoured by the presence of a small amount of starting PAA chains. These chains may come from PAA-**I** 6 (i), PAA chains resulting from the cleavage of the trithiocarbonate moiety of PAA-**I** 6 either by degradation (if any) during the emulsion step (ii) or during the methylation before SEC analysis of PAA-**I** 6 chains that did not participate to the emulsion step (iii). The

very low corresponding signal observed by SEC analyses cannot however be used to determine the molar mass with enough accuracy to tell which of these three assumptions is more probable.

Table 2. RAFT emulsion polymerization of S and BA mediated by PAA-**I** 6

Entry	Macro-CTA/M	t (h)	$DP_{n,th}$	Conv ^a (%)	M_{nSEC}^b (g mol ⁻¹)	\bar{D}^b	D_h^c	Poly ^c	D_n	D_w/D_n^d
L2	PAA- I 6/S	8	500	60	39,500	1.6	50	0.19	43	1.11
L4	PAA- I 6/S	8	900	70	62,500	1.7	65	0.13	60	1.09
L6	PAA- I 6/BA	8	550	60	39,700	1.7	34	0.19	30	1.21

^aMonomer conversion was determined gravimetrically. ^bNumber-average molar mass and dispersity were determined by SEC in THF after methylation using PS standards. ^c D_h were obtained by dynamic light scattering (DLS). ^d D_w/D_n were obtained by transmission electron microscopy. T = 80°C; pH = 3.1.

To further confirm the formation of block copolymers latexes were analysed by TEM. In all cases, assembled structures with a spherical morphologies ($D_n < 45$ nm) were observed. Micrographies of self-assembled block copolymers PAA-*b*-PS-*b*-PAA and PAA-*b*-PBA-*b*-PAA are shown in Figure 3. In this last case a cryo-TEM was used to preserve original morphology of nanoparticles. Additional illustrative images are also presented in Figure S6 (Table 2, Entries 1-3) are presented in Figure S6. As expected, the average diameter D_h obtained by DLS (Table 2) are slightly higher than those obtained by TEM due to the swelling of the PAA segment in water. The small particle sizes obtained although slightly broadly distributed either by TEM or DLS measurements (lower than 43 and 51nm respectively) were in agreement with the self assembly of block copolymers.

Besides, the amphiphilic block copolymer PAA-*b*-PS-*b*-PAA isolated from L2 was further analyzed by ¹H NMR. As it can be observed in the Figure 4a, the ¹H NMR spectrum (300 MHz) of the block copolymer recorded in DMSO-*d*₆ exhibited resonances corresponding to the phenyl groups of the PS segment between 7.3 and 6.2 ppm. PAA methyne protons of the main chains can be found between 2.1 and 2.4 ppm, while main chain methylene protons were between 1.2 and 2.0 ppm. The methyl proton signal of the alkoxyamine can be seen at 0.8 ppm and the signal associated to the methyne proton in position α to the oxygen atom of the alkoxyamine was found at 5.2 ppm. Figure 4b shows the ¹H NMR spectrum of the same product under the form of a latex dispersed in D₂O. The corresponding spectrum is indeed meant to give selective information about any water solvated species.³² In this case only the PAA signals (between 2.1 and 2.4 ppm and 1.2 and 2.0 ppm) and other peaks at 0.9 ppm associated to the methyls

of the alkoxyamine groups were observed. Since PS segments are no longer soluble in D₂O, the associated aromatic resonances disappeared. Only a very weak and broad signal remains suggesting that a few styrene units were slightly solvated by water at the interface and therefore became somewhat mobile because the attached hydrophilic PAA segments.³² The presence of these resonances in water may also be assigned to the alkoxyamine moieties carried by the PAA segments. The resonance of the methyl groups of the alkoxyamines are indeed still observed at around 1.0 ppm. These last results are in agreement with the formation of particles stabilized by the PAA hydrophilic segments. They further suggest that alkoxyamine moieties seemed to be present at least partly in water and thus accessible for further chemistry.

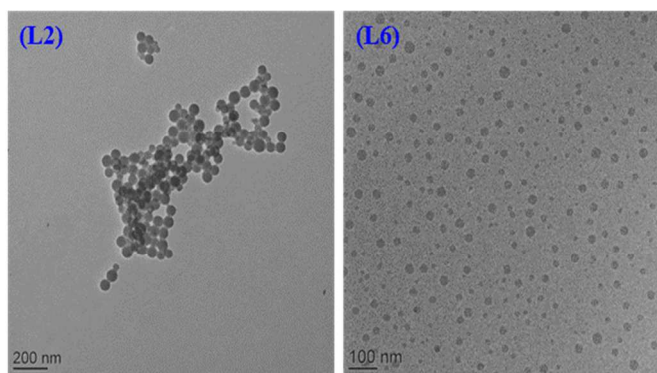


Figure 3. TEM images of latex L2 and cryo-TEM images of latex L6.

The chain-end functionalization of homopolymers and triblock copolymers prepared in solution departing from **I** was clearly demonstrated in our recent paper.²² Here we showed that the alkoxyamine end-group of poly(acrylic acid) blocks

can keep their integrity during the RAFT chain extension reaction (Scheme 2) with hydrophobic monomers if the temperature (80 °C) is kept below the cleavage temperature of the considered TEMPO-based alkoxyamines (ca 120°C). Consequently, latex particles as shown in Scheme 1 containing trithiocarbonate moieties (green dots) in their hydrophobic core and PAA chains end-capped with alkoxyamines (yellow dots) as hydrophilic shell.

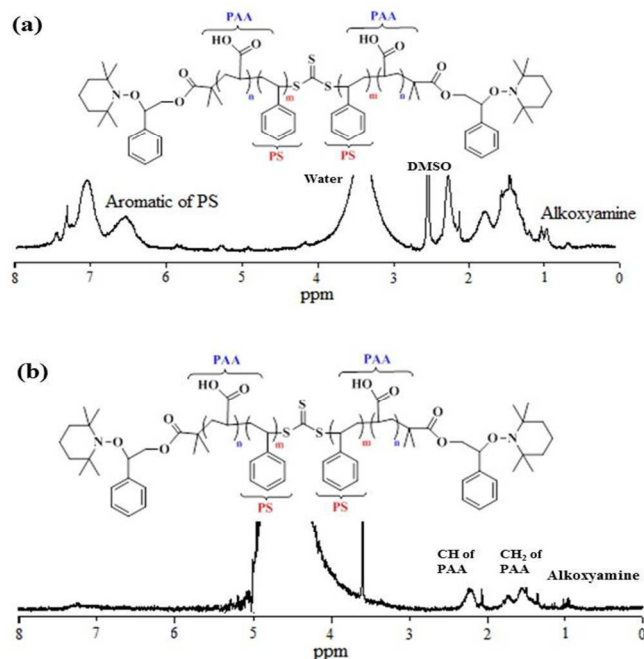


Figure 4. (a) ^1H NMR of latex L2 in DMSO, (b) ^1H NMR of Latex L2 in D_2O

3.3 Surface Initiated Polymerization from latex nanoparticles (Step 3)

Prior any surface initiated polymerization using the latexes synthesized above, we evaluated the potential of these latexes to undergo further polymerization involving both the alkoxyamine and the trithiocarbonate moiety simultaneously using a hydrophobic monomer. The motivation in these preliminary experiments was an original way to target multiblock copolymers in dispersed media. L6 (PAA-*b*-PBA-*b*-PAA block copolymer particles, $M_{n,SEC} = 39,700 \text{ g mol}^{-1}$; $D = 1.7$) which was prepared with from PAA-*I* 6 ($M_{n,SEC} = 8,040 \text{ g mol}^{-1}$; $D = 1.2$) (see Table 1), was used for S polymerization performed in water at 130 °C under pressure (3 bars) without the help of any additional initiator ($[S]/[L6] = 500$, see Table S1 for additional information). The corresponding successful polymerization is not a sign that alkoxyamines act as sole initiators in this system since thermal self-initiation of styrene cannot be ruled out. In addition, swelling of the particles with styrene will occur and involvement of the trithiocarbonate

groups cannot be neglected. The size of the particles (see Table S1) increased from 34 nm (L6) to 120 nm (L-NMP). The rather important increase in size cannot be assigned solely to surface-chain extension with styrene. The growth of PS block from the alkoxyamine in water may lead to some extent to destabilization and aggregation of the latex particles, resulting in larger objects. However the resulting aggregates remained stabilized by the PAA hydrophilic segments. The stability of the resulting latex was indeed followed over a year (Figure 5a). Besides, the formation of high Tg hydrophobic PS chains ($T_g \sim 100^\circ\text{C}$) is beneficial to TEM analysis. The M_n of the methylated polymer after polymerization was $45,000 \text{ g mol}^{-1}$ ($D = 1.8$) while the starting M_n was $39,700 \text{ g mol}^{-1}$ ($D = 1.3$). The shift in molar mass observed and the rather low molar mass obtained is not consistent with a conventional free radical polymerization of styrene and suggest the involvement of the alkoxyamine and/or the trithiocarbonate moieties. Admitting the RAFT and NMP were activated simultaneously the theoretical expected structure of this reaction is a heptablock copolymer. However, the obtained structure cannot be determined with accuracy as the styrene polymerization partition is unknown. Furthermore, the rather low thermal stability of the trithiocarbonate moiety and phenomena such as alkoxyamine entering the core of the particles after chain extension with styrene and potentially reacting with the chains growing inside the core could dramatically limit the elucidation of the exact structure.

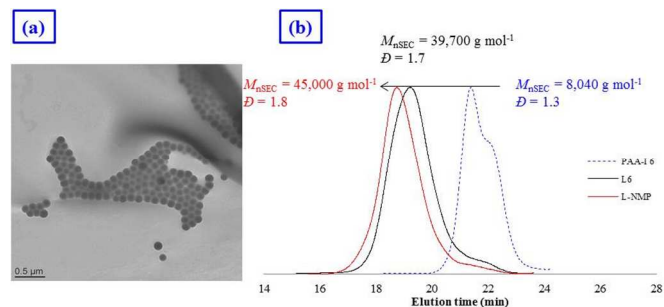


Figure 5. (a) Illustrative TEM images of corresponding latex (L6) after polymerization of styrene. (b) SEC traces of PAA-*I*, PAA-*b*-PBA-*b*-PAA (L6), and the copolymers obtained in L-NMP.

To exploit the reactivity of the surface alkoxyamines, a surface initiated polymerization (SIP) was tentatively performed in water by adding SSNa to the latex L2 (PAA-*b*-PS-*b*-PAA) and heating the resulting dispersion at 130°C under pressure *ca.* 3 bars with agitation.

NMP can indeed be undertaken independently from RAFT provided that the monomer to be polymerized is highly water soluble. The trithiocarbonate groups inside the hydrophobic core should then not disturb the SIP.

Considering that, as far as we know, there was no report on NMP-SIP performed in water, experiments (Table S1) were carried out with SSNa. A blank polymerization was also performed in absence of monomer. The latexes obtained after SIP (Latex NMP 1-3) were dialysed to quantify the SSNa residual monomer and thus its conversion. In all cases, any noticeable change in the latex aspect was observed; the latex exhibited a typical light scattering blue colour before and after reaction. The latexes were characterized by DLS, SEM and TEM to determine the average diameter and the morphologies of particles resulting from SIP. Samples were taken, diluted (< 1% of solids content) and placed in copper plate and grids for SEM and TEM observation respectively. The DLS analysis of latexes L2 and NMP-1 shown in Figure S7 indicates that the average diameter of nanoparticles increases from 50 to 72 nm. As recently reported,³³ this result may confirm that during the surface initiated polymerization a new PSSNa block is introduced initial triblock copolymer PAA-*b*-PS-*b*-PAA.

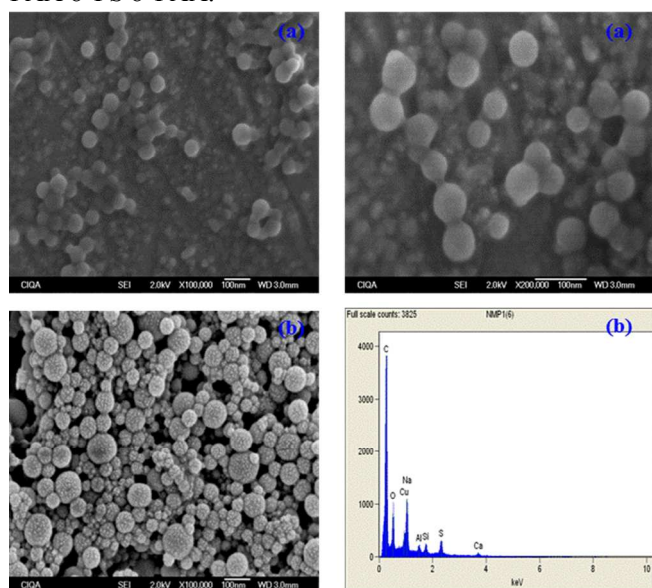


Figure 6. (a) SEM images of soft latex (L2), (b) SEM-EDX of latex NMP-1 (rough surface) obtained via SIP.

As it can be seen in Figure 6, the effect of SSNa polymerization is noticeable in the morphology of latex considering different conversions. At 20% of conversion, the surface of the particles previously soft (Figure 6a) was changed to rough surface (Figure 6b) with some dotted attributed to short chain of PSSNa. The SEM-EDX analysis of sample Latex NMP-1 (Figure 6b) indicated that sulphur, probably originating from SSNa units was present besides carbon, oxygen, and others elements such as copper (from the plate), Al and Si (possibly related to impurities), Na and Ca (from water).

By increasing the conversion of SSNa to 40%, the initial spherical particles from latex 2 were reorganized in the form interconnected nanofibers - the diameter of which is slightly larger than that of initial nanoparticles - together with some vesicles (Figure 7a). The blank experiment performed in absence of SSNa (i.e. thermal treatment) does not show any change in morphology (Figure 7b) and confirms that the SIP of SSNa is involved in the new obtained morphologies. It is worth recalling here that these nanoobjects are composed of self-assembled amphiphilic multiblock copolymers. For amphiphilic diblock copolymers, varying the relative volume fractions of each block usually dictates the final copolymer morphology, although kinetically trapped morphologies are quite common.^{34,35} The unexpected switch in morphology observed here can indeed be rationalized by both a change in the hydrophilic/lipophilic balance from PAA-*b*-PS-*b*-PAA copolymers to the formed PSSNa-*b*-PAA-*b*-PS-*b*-PAA-*b*-PSSNa block copolymers and the softening of the polystyrene core at 130°C. At the best of our knowledge it is the first time a NMP-SIP of SSNa is initiated from the surface of a latex. Besides, the morphology switch has been largely depicted in PISA system^{18,19} by increasing the hydrophobe fraction of self-assembled amphiphilic diblock copolymers. One could expect that the polymerization of SSNa should cause an increase in the hydrophilic volume fraction, which would favour spherical particles and not a sphere-to-cylinder transition. Although these preliminary results will require an in-depth investigation, they seem to show that such morphology switch can be triggered from the surface of the particles by softening the hydrophobic block and modifying the hydrophilic/hydrophobic balance of amphiphilic multiblock copolymers.

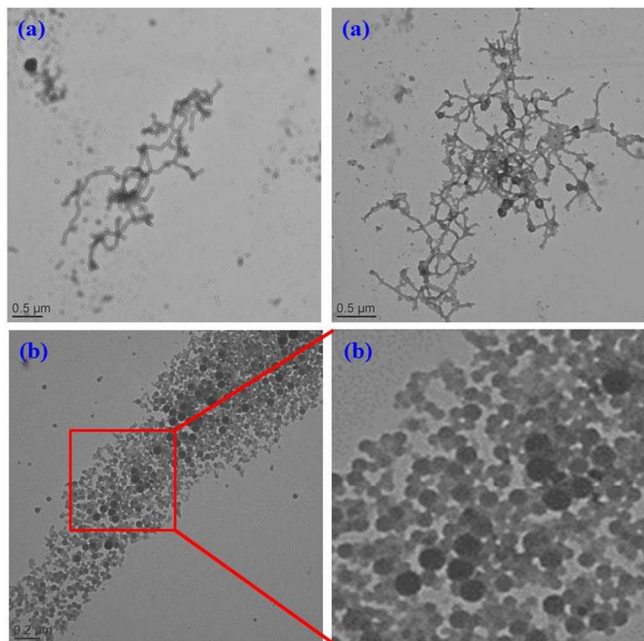


Figure 7. TEM images of latexes: (a) NMP-3, polymerization of SSNa via SIP, and (b) from blank experiment without SSNa.

Conclusions

I, a new symmetrical trithiocarbonate holding two alkoxyamine moieties, has been successfully used to control the RAFT polymerization of acrylic acid. The resulting PAA macro RAFT carrying a central trithiocarbonate group and two alkoxyamines at both chain ends were used in water to polymerize styrene and *n*-butyl acrylate using PISA. Well-defined latex nanoparticles decorated with alkoxyamine groups were produced. The polymerization of styrene in the presence of such latexes was performed. Multiblock structures resulting from both NMP and RAFT involving alkoxyamines and trithiocarbonates could not be evidenced although the involvements of these controlling moieties in the polymerization was suggested by the low molar mass of the final copolymers. Reactivation of the surface alkoxyamines at high temperature in the presence of styrene led to simultaneous NMP and RAFT at the surface and at the core of the particles leading to PS-*b*-PAA-*b*-PS-*b*-PBA-*b*-PS-*b*-PAA-*b*-PS multiblock copolymer particles. When SSNa was employed, surface initiated polymerization only occurred. A reorganization of the resulting PSSNa-*b*-PAA-*b*-PS-*b*-PAA-*b*-PSSNa amphiphilic multiblock copolymers into nanofibers was observed and possibly favoured by the modification of the hydrophilic/hydrophobic balance of the block copolymer and the reaction temperature. The reactive particles described in this paper represent a new platform to prepare a variety of new latexes.

Acknowledgements

Acknowledge is given to CONACYT for, scholarship of CST and project fund CB-2008-01-101637. Also thanks are given to: Hortensia Maldonado-Textle, Judith N. Cabello-Romero, Guadalupe Tellez-Padilla, Jesus Angel Cepeda-Garza, Omar García-Valdez (CIQA), Drs. Xuewei Zhang, Julien Parvole, and Edgar Espinosa (UMR, 5265, C2P2) and Prof. Bernadette Charleux (C2P2) for initiating the collaboration between the two groups. The help of Olivier Boyron (C2P2) on SEC analyses is greatly acknowledged.

Notes and references

^a Department of Polymer Chemistry, Centro de Investigacion en Quimica Aplicada, 140 Blvd. Enrique Reyna, Saltillo, Coahuila, 25294 Mexico, ramiro.guerrero@ciqa.edu.mx, Tel. +52 844 4389830 ext. 1238.

^b Laboratoire de Chimie Catalyse Polymères et Procédés (C2P2), Université de Lyon 1, CPE Lyon, CNRS UMR 5265, Team LCPP, Bat 308F, 43 Bd du 11 Novembre 1918, F-69616 Villeurbanne, France, franck.dagosto@univ-lyon1.fr

† [Electronic Supplementary Information \(ESI\) available:](#) [Kinetic follow: SEC traces of PAA-*I* synthesized through RAFT polymerization mediated by *I*; SEC traces of PAA-*I* 2 and its corresponding cleaved product, SEC traces of PMA-*I* before and after an ‘useless’ methylation, ¹HNMR corresponding to sample PAA-*I* 6 synthesized through RAFT polymerization mediated by *I*; Conversion vs time and Conversion vs $M_{n,SEC}$ corresponding to kinetic follow of block copolymerization (L4 and L6); TEM images revealing the spherical nano-structure of latexes, DLS chromatograms of L2 and Latex NMP-1]. See DOI: 10.1039/b000000x/

¹ A. D. Jenkins, R. G. Jones, and G. Moad, *Pure Appl. Chem.*, 2010, **82**, 483–491

² M. K. Georges, R. P. N. Veregin, P. M. Kazmaier, and G. K. Hamer, *Macromolecules*, 1993, **26**, 2987–2988

³ C. J. Hawker, A. W. Bosman, and E. Harth, *Chem. Rev.*, 2001, **101**, 3661–3688

⁴ J. Nicolas, Y. Guillauneuf, C. Lefay, D. Bertin, D. Gigmes, and B. Charleux, *Prog. Polym. Sci.*, 2013, **38**, 63–235

⁵ K. Matyjaszewsky, and J. Xia, *Chem. Rev.*, 2001, **101**, 2921–2990

⁶ K. Matyjaszewsky, *Macromolecules*, 2012, **45**, 4015–4039

⁷ E. Rizzardo, G. Moad, and S. H. Thang, US Patent, WO 98/01478

⁸ J.-J. Chiefari, Y. K. Chong, F. Ercole, J. Krstina, J. Jeffery, T. P. T. Le, R. T. A. Mayadunne, G. F. Meijs, C. L. Moad, G. Moad, E. Rizzardo, and S. H. Thang, *Macromolecules*, 1998, **31**, (16), 5559–5562

⁹ G. Moad, E. Rizzardo, and S. H. Thang, *Aust. J. Chem.*, 2012, **65**, 985–1076

¹⁰ M. Destarac, *Macromol. React. Eng.*, 2010, **4**, 165–179

¹¹ M. F. Cunningham, *Prog. Polym. Sci.*, 2008, **33**, 365–398

- ¹² P. B. Zetterlund, Y. Kagawa, and M. Okubo, *Chem. Rev.*, 2008, **108**, 3747–3794
- ¹³ A. Darabi, A. R. Shirin-Abadi, J. Pinaud, P. G. Jessop, and M. F. Cunningham, *Polym. Chem.*, 2014, **5**, 61631–6170
- ¹⁴ H. Maehata, X. Liu, M. Cunningham, and B. Keoshkerian, *Macromol. Rapid Commun.*, 2008, **29**, 479–484
- ¹⁵ A. R. Szkurhan, and M. K. Georges, *Macromolecules*, 2004, **37**, 4776–4782.
- ¹⁶ M. J. Monteiro, and M. F. Cunningham, *Macromolecules*, 2012, **45**, 4939–4957
- ¹⁷ C. J. Ferguson, R. J. Hughes, D. Nguyen, B. T. T. Pham, R. G. Gilbert, A. K. Serelis, C. H. Such, and B. S. Hawket, *Macromolecules*, 2005, **38**, 2191–2204
- ¹⁸ B. Charleux, G. Delaître, J. Rieger, and F. D'Agosto, *Macromolecules*, 2012, **45**, 6753–6765
- ¹⁹ Nicholas J. Warren and Steven P. Armes, *J. Am. Chem. Soc.*, 2014, **136**, 10174–10185
- ²⁰ Y. Mai and A. Eisenberg, *Chem. Soc. Rev.*, 2012, **41**, 5969–5985
- ²¹ X. Zhang, S. Boissé, W. Zhang, P. Beaumier, F. D'Agosto, J. Rieger, and B. Charleux, *Macromolecules*, 2011, **44**, 4149–4168.
- ²² C. St Thomas, H. Maldonado-Textle, J. Cabello-Romero, J. Macossay, N. Esturau-Escofet, X. Zhang, and R. Guerrero-Santos, *Polym. Chem.*, 2014, **5**, 3089–3097.
- ²³ C. St Thomas, H. Maldonado-Textle, A. Rockenbauer, L. Korecz, N. Nagy, and R. Guerrero-Santos, *J. Polym. Sci. Part A: Polym. Chem.*, 2012, **50**, 2944–2956
- ²⁴ L. Couvreur, C. Lefay, J. Belleney, B. Charleux, O. Guerret, and S. Magnet, *Macromolecules*, 2003, **36**, 8260–8267
- ²⁵ I. Chaduc, M. Girod, R. Antoine, B. Charleux, F. D'Agosto, and M. Lansalot, *Macromolecules*, 2012, **45**, 5881–5893
- ²⁶ I. Chaduc, A. Crepet, O. Boyron, B. Charleux, F. D'Agosto, and M. Lansalot, *Macromolecules*, 2013, **46**, 6013–6023
- ²⁷ M. F. Llauro, C. Lavadière, J. Loiseau, F. Boisson, F. Delolme, and J. Claverie, *J. of Polym. Sci. Part A: Polym. Chem.*, 2004, **42**, 5439, 5462
- ²⁸ J. Loiseau, N. Doërr, J. M. Suau, F. B. Egraz, M. F. Llauro, C. Lavadière, and J. Claverie, *Macromolecules*, 2003, **36**, 3066–3077
- ²⁹ C. J. Fergusson, R. J. Hugues, B. T. T. Pham, B. S., Hawket, R. G. Gilbert, A. K. Serelis, and C. H. Such, *Macromolecules*, 2002, **35**, 9243–9245
- ³⁰ C. Schmid, S. Weidner, J. Falkenhagen, and C. Barner-Kowollik, *Macromolecules*, 2012, **45**, 87–99
- ³¹ I., Lacík, M., Stach, P., Kasák, V., Semak, L., Uhelská, A., Chovancová, G., Reinhold, P., Kilz, D., Delaître, B., Charleux, I., Chaduc, F., D'Agosto, M., Lansalot, M., Gaborieau, P., Castignolles, R. G., Gilbert, Z., Szablan, C., Barner-Kowollik, P., Hesse, and M., Buback, *Macromol. Chem. Phys.*, 2015, **216**, 23–27
- ³² F. D'agosto, M.-T. Charreyre, C. Pichot, and R. G. Gilbert, *J. Polym. Sci. Part A: Polym. Chem.*, 2003, **41**, 1188–1195
- ³³ H. Kang, Y. Su, X. He, S. Zhang, J. Li, and W. Zhang, *J. Polym. Sci. Part A: Polym. Chem.*, **2015**, DOI:10.1002/pola.27620
- ³⁴ D. E. Discher, and A. Eisenberg, *Science*, 2002, **297**, 967–973
- ³⁵ A. Blanazs, S. P. Armes, A. J. Ryan, *Macromol. Rapid Commun.*, 2009, **30**, 267–277.